The Effect of Cation Nonstoichiometry on the Electrical Conductivity of $CaZrO_3$

Soon Cheol Hwang[a,b] and Gyeong Man Choi[b,*]

[a]*New Materials & Components Research Center, Research Institute of Industrial Science & Technology, San 32, Hyoja-dong, Pohang 790-330, South Korea*

[b]*Department of Materials Science and Engineering, Pohang University of Science and Technology, San 31, Hyoja-dong, Pohang, 790-784, South Korea*

**Corresponding author*

Abstract

The electrical conductivities of $Ca_{1-x}ZrO_{3-\delta}$ systems were measured by using impedance spectroscopy as a function of Ca/Zr ratio ($0 \leq x \leq 0.1$) and temperature (550□~1100□). Stoichiometric $CaZrO_3$ revealed poor sinterability due possibly to the free CaO observed at grain junctions. With decreasing Ca/Zr ratio, the free CaO disappeared and the sintered density increased. The total electrical conductivity rapidly decreased, ~100 times at 1100□, when the Ca content decreased below 0.98. The impedance measurement revealed that the decrease is due mostly to the increase in the grain boundary resistivity. The activation energy of grain boundary resistivity also rapidly increased with decreasing Ca/Zr ratio. In other words, the grain boundary resistivity was very sensitive to Ca/Zr ratio. It is suggested that the single phase composition is near $Ca_{0.98}ZrO_3$.

Keywords : Nonstoichiometry, grain boundaries(B), electrical conductivity(C), impedance(C) perovskite(D),

1. Introduction

Solid state oxygen ion conductors with little electronic conductivity, high thermal stability, and good chemical inertness are required to measure oxygen potentials at high temperature and in various oxygen partial-pressure (Po_2). Calcium zirconate with a perovskite structure has the required high thermal and chemical stability, and the good thermal shock resistance.[1] $CaZrO_3$ is a mixed p-type and oxygen ionic conductor in high Po_2 but a stable ionic conductor in low Po_2.[2-5] It exhibits protonic conduction under hydrogen-containing atmosphere at elevated temperature, if the zirconium in the oxides was partially replaced by aliovalent cations.[6-8] Thus it has been used as a refractory material, a microwave dielectric, a solid electrolyte and a proton conductor.[9-10] However, the phase homogeneity region for this compound has been reported to be very narrow. Thus, there are still controversies regarding to the electrical conductivity as a function of Ca/Zr ratio.[11-12]

In this study, the electrical conductivities of $Ca_{1-x}ZrO_{3-\delta}$ systems were investigated as a function of Ca/Zr ratio ($0 \le x \le 0.1$) and temperature (550□~1100□). The phase composition was characterized by the XRD (X-ray diffraction) analysis and SEM observation. The electrical conductivity was measured by using impedance spectroscopy. From the conductivity measurements, the effects of cationic nonstoichiometry on the electrical property of calcium zirconate were discussed.

2. Experimental procedure

$Ca_{1-x}ZrO_{3-\delta}$ ($0 \le x \le 0.1$) ceramics were prepared by a conventional solid state reaction method. $CaCO_3$ (99.9%, Showa, Japan) and ZrO_2 (99.9%, Tosoh, Japan) powders were used as the starting materials. The oxides, mixed by ball milling for 24h, were calcined at 1350□ for 4h. The calcined powders were analysed by X-ray diffractometry (Model D-MAX 1400, Rigaku, Japan) to confirm the formation of the perovskite phase. The calcined powders were isostatically pressed into pellets at a pressure of 200□, followed by sintering at 1700□ for 4h in air. The microstructures of fractured surface were examined by FE-SEM (Model S-4300SE, Hitachi, Japan). Specimens for electrical measurements were prepared from sintered pellets by polishing the faces flat. The platinum-paste electrodes (Engelhard model #6926) were fired at 1000□ for 1h. The two-probe a.c. measurement technique was used to obtain the electrical resistance. The impedance in the frequency range between 5□ to 13□ was obtained by LF Impedance analyzer (Model 4192A, Hewlett-Packard, USA). The temperature dependence of electrical conductivity was measured between 550□ and 1100□ in dry air.

3. Results and discussion

The XRD patterns of the calcined $Ca_{1-x}ZrO_{3-\delta}$ ($0 \le x \le 0.1$) powders are shown in Fig. 1 and SEM micrographs of fractured surface of sintered specimens are shown in Fig. 2. As shown in Fig. 1, only the single phase $CaZrO_3$ peaks were obtained for $0 \le x \le 0.02$ compositions. However for $x \ge 0.03$, the excess ZrO_2 (tetragonal) peaks were found in this systems. As x increases above 0.03, the intensity of the excess zirconia peaks gradually increased. Fig. 2 shows the CaO-rich phase (in the circle) for samples with x=0 and 0.01 compositions. For $x \ge 0.02$, the free CaO disappeared. The grain size of sintered specimen of $x \ge 0.02$ is slightly smaller than that of $x \le 0.01$ specimens. Although zirconia phase was shown by XRD, no second-phase zirconia was observed in the microstructure. Stoichiometric $CaZrO_3$ specimen revealed poor sinterability, ~ 93% relative density, and the sintered specimen collapsed into powders during storage in room atmosphere. The free CaO remained at grain junctions may be responsible for it. The CaO may have reacted with CO_2 and H_2O in room atmosphere and the subsequent volume expansion may have resulted in the collapse. With increasing x, the free CaO disappeared and the sintered density increased above 97% for $x \ge 0.02$. From the XRD and SEM observations, it is suggested that the single phase composition in calcium zirconate systems may lie near $Ca_{0.98}ZrO_3$.

The impedance spectra of $Ca_{1-x}ZrO_{3-\delta}$ specimen at 650□ in dry air for x=0.01, 0.013, 0.016 are shown in Fig. 3. The impedance spectra are composed of two partially overlapped semicircles. The values of the respective capacitance shows that the first semicicle at higher frequencies corresponds to the grain process, and the second semicircle at lower frequencies to the grain boundary process. The total conductivity(σ_t) of the specimen can be calculated from the total resistance(R_t), that is, the sum of grain resistance and grain boundary resistance. For x=0.01, the ratio of R_{gb} to R_g was ~ 4.3 at 650□ in dry air. The grain boundary resistance mostly determines the total resistance. With increasing x, the overlapping of two semicircles representing the grain and the grain boundary process becomes more severe. The overlapping was mainly due to the large and increasing grain boundary resistance. For all compositions, the change in grain resistance is small. Thus it is concluded that the grain boundary resistance mostly determines the specimen resistance in this figure.

Fig. 4 shows the temperature dependence of the electrical conductivity of $Ca_{1-x}ZrO_{3-\delta}$ specimen in air. The total conductivity of the specimen was obtained from the total resistance values on impedance spectrum. The activation energy(E_a) values, calculated by fitting the data, were also shown for each composition. It is clearly shown that σ_t of $Ca_{1-x}ZrO_{3-\delta}$ specimen decreases with increasing x up to x=0.03 with the corresponding increase of E_a (1.14 to 2.46 eV). For x above 0.03, σ_t slightly increased with the slight decrease of E_a (2.46 to 2.34 eV).

Fig. 5 shows the σ_t of $Ca_{1-x}ZrO_{3-\delta}$ specimen at 1000□ and 1100□ in air as a function of x. The entire composition range may be divided into two regions following the shape of curve and according to the XRD and the SEM observation. The boundary line may be drawn at x=0.02. Below x=0.02 where free CaO was observed, σ_t rapidly decreased with x, more than ~100 times. Above x=0.02, the conductivity change was small, it actually increased slightly.

Fig. 6 shows the comparison of the grain(σ_g) and the grain boundary conductivity(σ_{gb}) as a function of temperature for x=0 and x=0.013 of $Ca_{1-x}ZrO_{3-\delta}$ specimen in air. The deconvolution of grain and grain boundary semicircles was not possible for x above 0.013 since one large semicircle was only shown. The magnitude of σ_g and the E_a values were nearly the same (E_a=0.85, 0.86 for x=0 and x=0.013, respectively). However, the σ_{gb} and E_a shows a large difference between two compositions (E_a=1.20, 1.44 for x=0 and x=0.013, respectively). In other words, the σ_{gb} is very sensitive to Ca/Zr ratio in contrast to σ_g. It is again apparent that σ_t was mainly determined by σ_{gb}. The magnitude and E_a values of σ_t (E_a=1.14, 1.36 for x=0 and x=0.013, respectively) is very close to those of σ_{gb} (E_a=1.20, 1.44 for x=0 and x=0.013, respectively) for both samples. Since the linear relation of log σ_t vs. 1/T continues up to 1100□, the grain boundary contribution to the total resistance does not seem to disappear with temperature. In other words, the σ_t is mostly determined by σ_{gb} even at high temperature. Dudek and Bucko[12] suggested the introduction of excess calcia into calcium zirconate generates oxygen vacancies and thus significantly enhances electrical conductivity. However, in this study, the σ_g was found to be nearly insensitive to x. Thus the substitution of calcia in zirconium site is

very limited. The free CaO and the excess zirconia may act as a role to change the grain boundary composition. The insulating grain boundary is responsible for the high sample resistance. Further study is necessary for the origin of grain boundary resistance.

4. Conclusions

The electrical conductivities of $Ca_{1-x}ZrO_{3-\delta}$ systems were investigated as a function of Ca/Zr ratio ($0 \le x \le 0.1$) and temperature (550□~1100□). From the XRD and microstructure observations, it is suggested that the single phase composition in calcium zirconate system may lie near $Ca_{0.98}ZrO_3$. For $0 \le x \le 0.02$, the total electrical conductivity rapidly decreased with x. The activation energy of grain boundary resistivity also increased with x. The sample resistance was mainly determined by the grain boundary resistance.

Acknowledgement

The authors are grateful for the financial support from POSCO, Korea.

5. References

1. Longo, V., Marchini, F., Ricciardiello, F., de Pretis, A., CaZrO3-based ceramics. A proposal for the choice of starting materials. *La Ceramica*, 1981, **34**, 23-28

2. Longo, V., Ricciardiello, F., New compositions in the solid solution of alkaline earth zirconates : electrical properties and thermal shock resistance. *Silicates Industriels*, 1981, **1**, 3-7

3. Fischer, W. A., Janke, D., Schulenburg, M., Calcium zirconate as solid electrolyte at temperatures around 1600□. *Arch. Eisenhuttenwesen*, 1976, **47**, 525-30

4. Wang, C., Xu, X., Yu, H., Wen, Y. and Zhao, K., A study of the solid electrolyte Y_2O_3-doped $CaZrO_3$. *Solid State Ionics*, 1988, **28-30**, 542-545

5. Pandit, S. S., Weyl, A., Janke, D., High-temperature ionic and electronic conduction in zirconate and hafnate compounds. *Solid State Ionics*, 1994, **69**, 93-99

6. Yajima, T., Kazeoka, H., Yogo, T. and Iwahara, H., Proton conduction in sintered oxides based on CaZrO3. *Solid State Ionics*, 1991, **47**, 271-275

7. Iwahara, H., Yajima, T., Hibino, T., Ozaki, K. and Suzuki, H., Proton conduction in calcium, strontium and barium zirconates. *Solid State Ionics*, 1993, **61**, 65-69

8. Kurita, N., Fukatsu, N., Ito, K. and Ohashi, T., Proton conduction domain of indium-doped calcium zirconate. *J. Electrochem. Soc.*, 1995, **142**, 1552-1559

9. Yajima, T., Koide, K., Takai, H., Fukatsu, N., Iwahara, H., Application of hydrogen sensor using proton conductive ceramics as a solid electrolyte to aluminum casting industries. *Solid State Ionics*, 1995, **79**, 333-337

10. Fukatsu, N., Kurita, N., Koide, K., Ohashi, T., Hydrogen sensor for molten metals usable up to

1500K. *Solid State Ionics*, 1998, **113-115**, 219-227

11. Rog, G., Dudek, M., Kozlowska-Rog, A., Bucko, M., Calcium zirconate : preparation, properties and application to the solid oxide galvanic cells. *Electrochimica Acta*, 2002, **47**, 4523-4529

12. Dudek, M., Bucko, M., Electrical properties of stoichiometric and non-stoichiometric calcium zirconate. *Solid State Ionics*, 2003, **157**, 183-187

Figure captions

Fig. 1. XRD patterns of $Ca_{1-x}ZrO_{3-\delta}$ powders calcined at 1350□ for 4h.

Fig. 2. SEM micrographs of fractured surface of $Ca_{1-x}ZrO_{3-\delta}$ specimen sintered at 1700□ for 4h (bars=20□). (a) x=0 (b) x=0.01 (c) x=0.02 (d) x=0.05

Fig. 3. Impedance spectra of $Ca_{1-x}ZrO_{3-\delta}$ specimen at 650□ in air for x=0.01, 0.013, 0.016.

Fig. 4. The temperature dependence of the total (grain + grain boundary) electrical conductivity of $Ca_{1-x}ZrO_{3-\delta}$ specimen in air for $0 \leq x \leq 0.1$.

Fig. 5. The total electrical conductivity of $Ca_{1-x}ZrO_{3-\delta}$ specimen in air as a function of x.

Fig. 6. The comparison of the grain and the grain boundary conductivity as a function of temperature for x=0 and x=0.013 of $Ca_{1-x}ZrO_{3-\delta}$ specimen in air. The scale of the figure was the same as that of Fig. 4 for easy comparison.

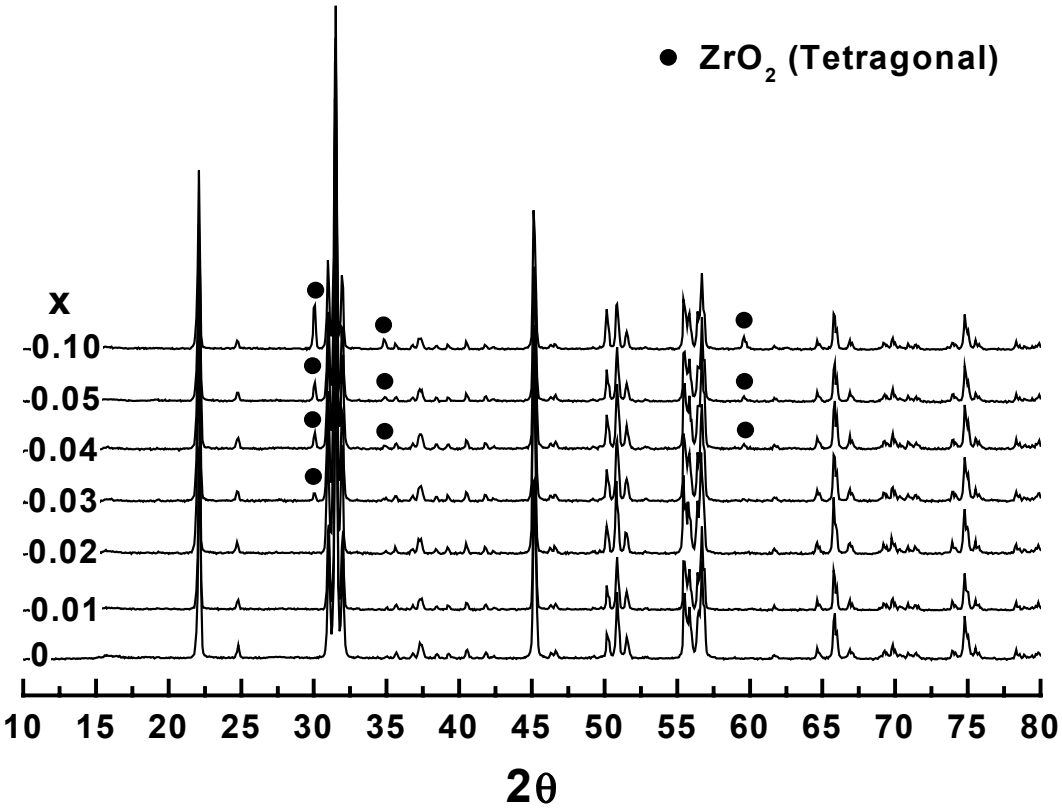
● ZrO2 (Tetragonal)
x
0.10
0.05
0.04
0.03
0.02
0.01
0
10 15 20 25 30 35 40 45 50 55 60 65 70 75 80
2θ

Fig.1.

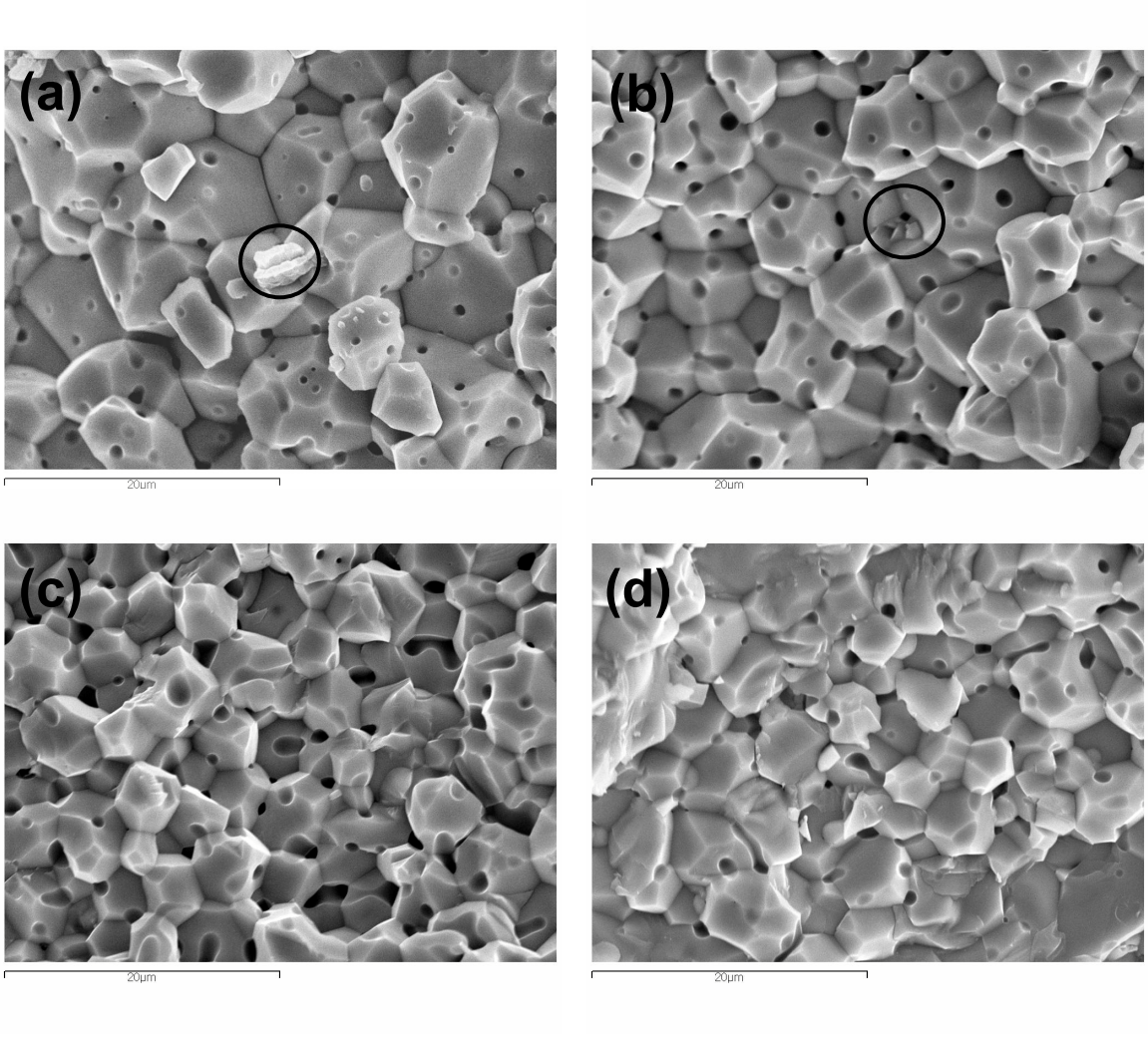

Fig.2.

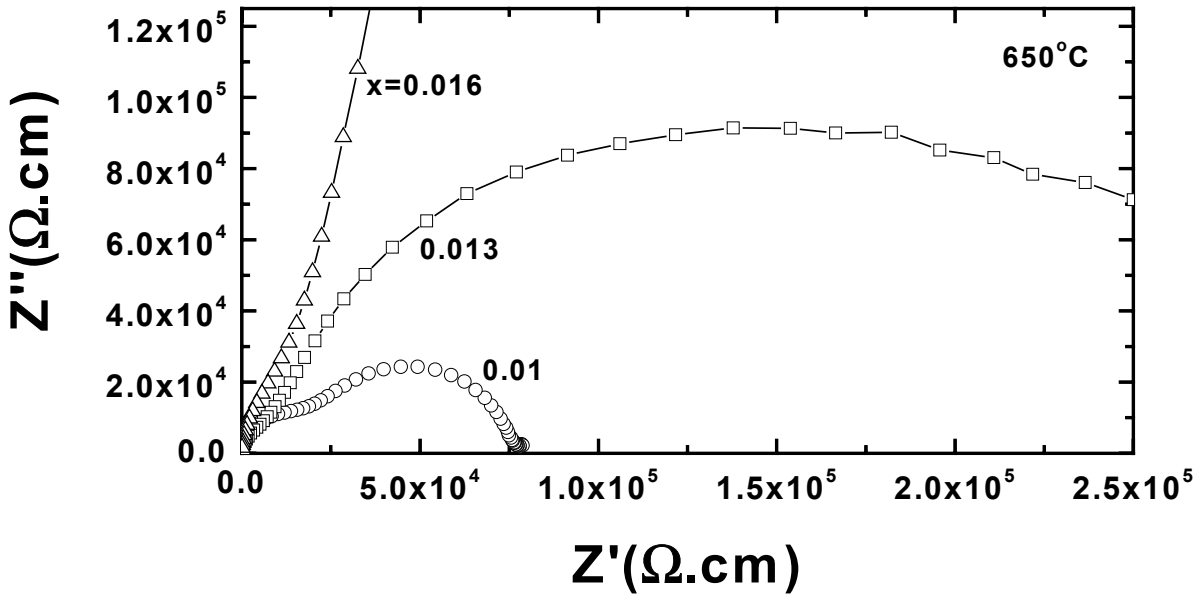
1.2x10^5
1.0x10^5
8.0x10^4
6.0x10^4
4.0x10^4
2.0x10^4
0.0
Z''(Ω.cm)
650°C
x=0.016
0.013
0.01
0.0
5.0x10^4
1.0x10^5
1.5x10^5
2.0x10^5
2.5x10^5
Z'(Ω.cm)

Fig.3

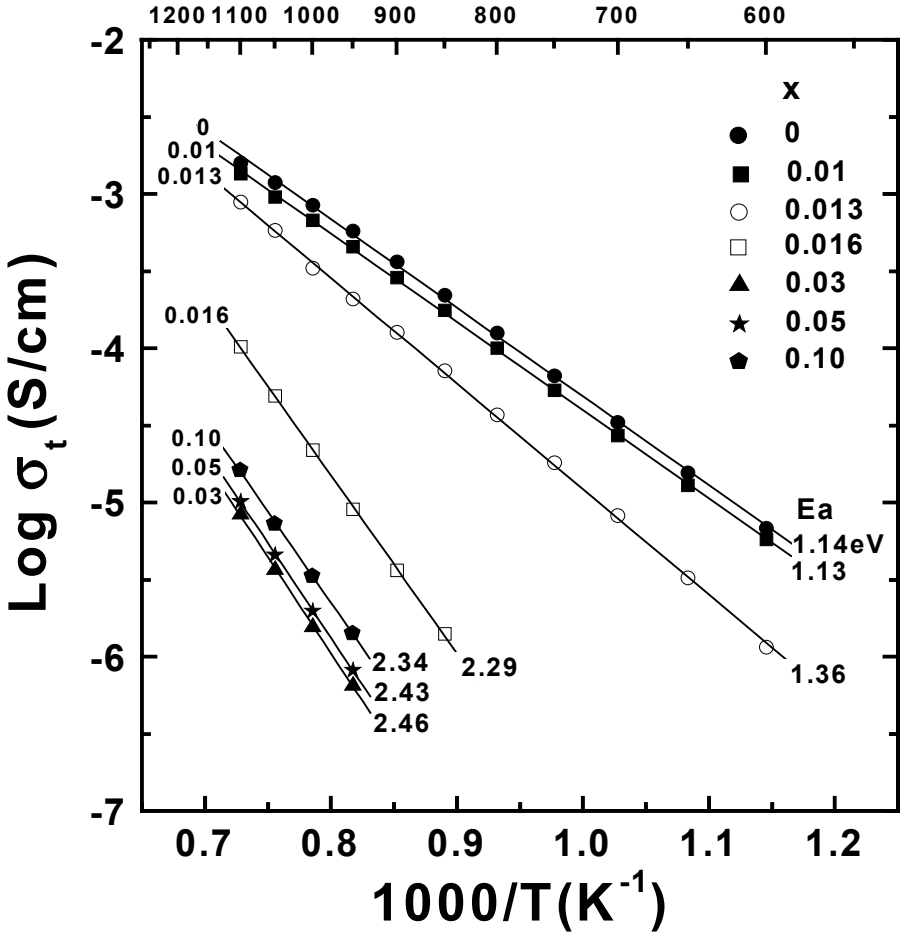
1200 1100 1000 900 800 700 600
-2
-3
-4
-5
-6
-7
Log σt (S/cm)
0.7 0.8 0.9 1.0 1.1 1.2
1000/T(K-1)
x
0
0.01
0.013
0.016
0.03
0.05
0.10
Ea
1.14eV
1.13
1.36
2.29
2.34
2.43
2.46

Fig.4

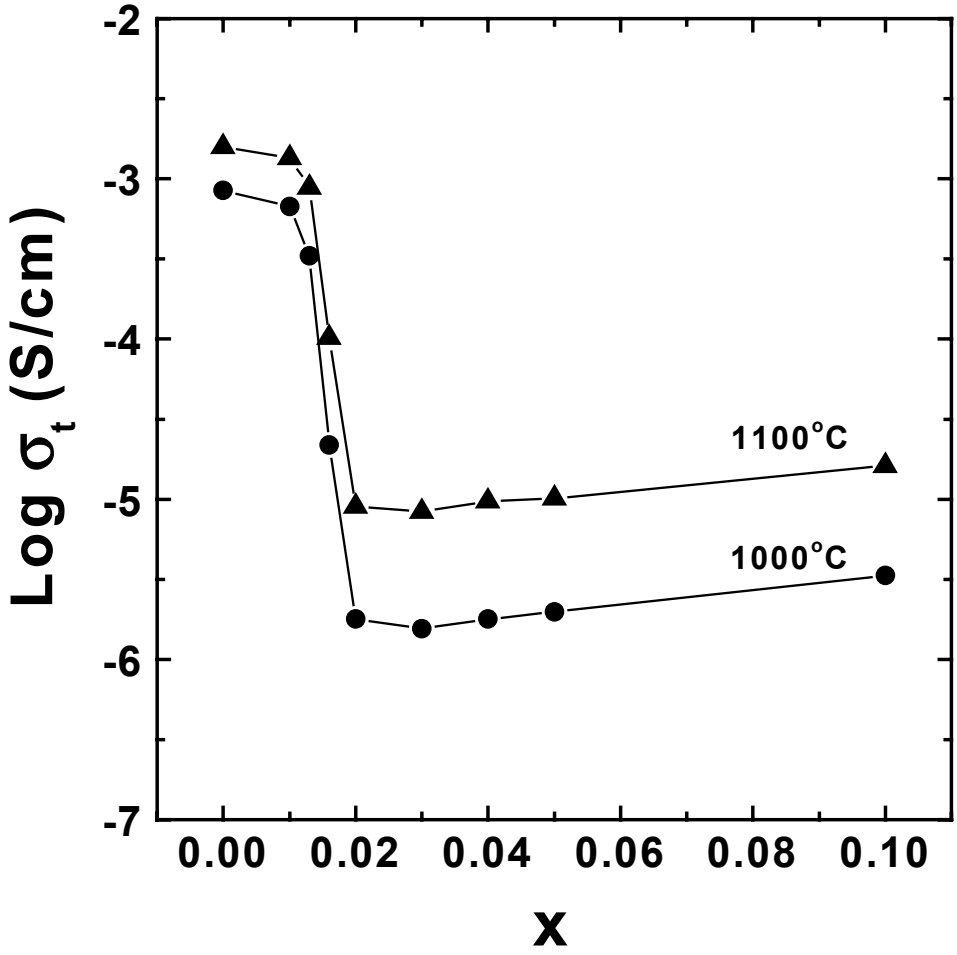

Fig.5

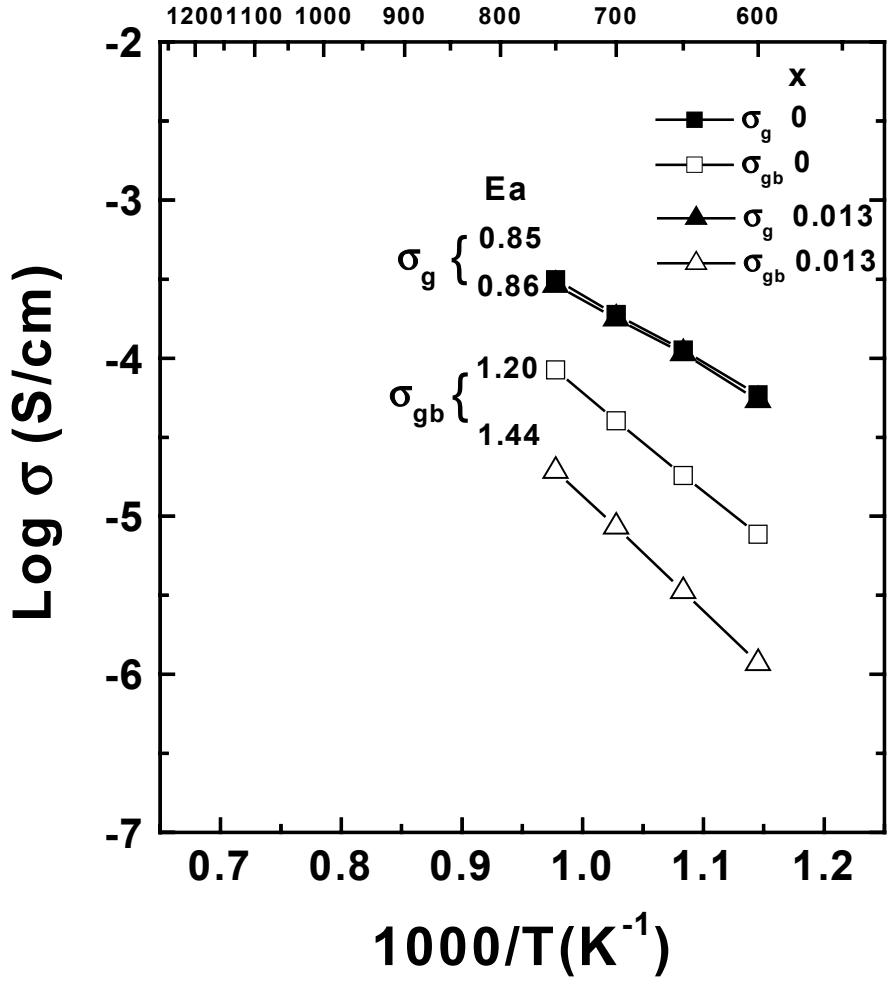
1200 1100 1000 900 800 700 600
-2
-3
-4
-5
-6
-7
Log σ (S/cm)
0.7 0.8 0.9 1.0 1.1 1.2
1000/T(K-1)
x
σg 0
σgb 0
σg 0.013
σgb 0.013
Ea
σg { 0.85 0.86
σgb { 1.20 1.44

Fig.6